J Vis (2010) 13:7–16
DOI 10.1007/s12650-009-0006-5

REGULAR PAPER

Yan Rong Li · Satoshi Someya · Koji Okamoto

An experimental investigation of flow-induced acoustic resonance and flow field in a closed side branch system using a high time-resolved PIV technique

Received: 6 March 2009 / Revised: 15 July 2009 / Accepted: 15 September 2009 / Published online: 8 December 2009

Abstract Systems with closed side branches are liable to an excitation of sound known as cavity tone. It may occur in pipe branches leading to safety valves or to boiler relief valves. The outbreak mechanism of the cavity tone has been ascertained by phase-averaged pressure measurements in previous research, while the relation between sound propagation and the flow field is still unclear due to the difficulty of detecting the instantaneous velocity field. It is possible to detect the two-dimensional instantaneous velocity field using high time-resolved particle image velocimetry (PIV). In this study, flow-induced acoustic resonance in a piping system containing closed side branches was investigated experimentally. A high time-resolved PIV technique was used to measure the gas flow in a cavity. Airflow containing oil mist as tracer particles was measured using a high-frequency pulse laser and a high-speed camera. The present investigation on the coaxial closed side branches is the first rudimentary study to visualize the fluid flow two-dimensionally in a cross-section using high time-resolved PIV, and to measure the pressure at the downstream side opening of the cavity by microphone. The fluid flows at different points in the cavity interact, with some phase differences between them, and the relation between the fluid flows was clarified.

Keywords Cavity tone · Acoustic resonance · Flow-induced vibration · Coaxial closed side branches · Visualization · Particle image velocimetry

List of symbols

C	The speed of sound when $T = 23°C$, $C = 345.3$ m/s (m/s)
d	The width of the branch (m)
D	The depth of the main pipe (m)
Ex	The difference between the measured frequency and the calculated one (%)
f_{CAL}	The frequency estimated from the empirical equation (Hz)
f_{MIC}	Dominant frequency of the pressure fluctuation by FFT (Hz)
f_{PIV}	Dominant frequency of the velocity fluctuation by FFT (Hz)
L	The length of the branch (m)
m	The acoustic mode order
M	Mach number
Q	Total flow rate (l/min)

Y. R. Li · S. Someya (✉) · K. Okamoto
Department of Human and Engineered Environmental Studies, Graduate School of Frontier Sciences,
University of Tokyo, 5-1-5 Kashiwanoha, Kashiwa, Chiba 277-8563, Japan
E-mail: some@some-ya.net
Tel.: +81-4-71365872
Fax: +81-4-71364603

S. Someya
National Institute of AIST, 1-2-1 Namiki, Tsukuba, Ibaraki 305-8564, Japan

S	The fluctuation rate at the mouth of the cavity
St_{MIC}	Strouhal number ($St_{MIC} = (f_{MIC})d/V_m$)
St_{PIV}	Strouhal number ($St_{PIV} = (f_{MIC})d/V_m$)
T	The room temperature of the laboratory (°C)
V	Mean velocity in the main pipe (m/s)
V_f	The propagation velocity of the fluctuation along the shear layer at the mouth of the cavity (m/s)
V_m	Local mean velocity at the mouth of the cavity (m/s)
V_r	The vertical component of the relative velocity (m/s)
V_y	The vertical component of the detected velocity vector in specific point (m/s)
$\bar{V}_y$	The time-averaged value of the vertical component of the detected velocity vector (m/s)
w	The thickness of the main pipe and the branch (m)

1 Introduction

Systems with closed side branch pipes are liable to an excitation of sound with discrete frequency components. East (1966) was one of the first researchers to report that fluid flow across the mouth of a deep rectangular cavity can cause the production of powerful acoustic tones. Numerous research groups including Coffman and Bernstein (1980), Baldwin and Simmons (1986), Bernstein and Bloomfield (1989), Bruggeman et al. (1989), and Kitajima et al. (2006) have investigated flow-induced acoustic vibration in closed side branches for a wide variety of practical applications, including natural gas, gas transport, steam piping systems, power stations, chemical plants, compressor installations, and other industrial applications. When high-velocity steam/gas passes safety relief valves, it may produce acoustic resonance in the valves and subsequent noise, excessive vibration. This phenomenon is undesirable in several engineering applications, because the induced sound can cause intense noise and considerable vibration in the surrounding mechanical structures. One of the first studies to deal with excessive vibration and valve failure explicitly was by Coffman and Bernstein (1980).

The airflow in the pipeline causes the excitation of acoustic oscillations at frequencies close to the eigenfrequencies of the branch. The energy exchange between the flow and acoustic modes of the resonator forms the flow-acoustic feedback loop. Rockwell and Naudascher (1978), Stoneman et al. (1988), Ziada (1994) and others have proposed that acoustic resonance of side branches is caused by a feedback excitation mechanism, which is referred to in the literature as a "fluid-resonant mechanism". The simple explanation of the mechanics of self-sustaining acoustic resonance in a side branch is summarized by Ziada and Shine (1999) as follows: the feedback is provided by the acoustic power of the resonant standing wave in the side branch. This pressure fluctuation induces new perturbations in the unstable shear layer at the separation point. As the shear layer perturbations are amplified and convected downstream, they interact with the acoustic field and produce acoustic energy that reinforces the resonance of the acoustic mode. Side branches are particularly liable to resonance, because the velocity of the resonance modes has its maximum amplitude at the location of the shear layer. This makes the excitation of the shear layer by the resonant acoustic mode as well as the interaction of the resulting shear layer oscillations with the resonant acoustic mode efficient.

The research on the vortex structure of the two-dimensional steady flow in a lid-driven rectangular cavity at different depth-to-width ratios and Reynolds numbers was carried out using a lattice Boltzmann method by Cheng and Hung (2006). Their results clarified the effects of the aspect ratio and Reynolds number on the size, center position and number of vortices. For $L/D \gg 1$, the center of the first large vortex (i.e., the biggest vortex near the edge of the cavity) located near to the downstream side of the cavity.

The previous works on the Strouhal number in which the resonances have the maximum amplitude by Jungowski et al. (1989) and Ziada and Bühlmann (1992) have suggested that: for the first hydrodynamic mode of the shear flow oscillation which corresponding to one vorticity (one node) in the shear layer along the mouth of the cavity, St, varied between 0.27 and 0.55 for a given range of diameter ratio. The acoustic modes of the branch subsystem are excited consecutively, as the flow velocity in the main pipe is increased.

Maguire (1985), Erickson et al. (1986), Karagoz (1993), Ziada (1994), and Dequand et al. (2003) have visualized the excitation of resonance. Ziada (1994) investigated the coupling of the shear layer with the sound field of a resonant side branch using smoke under forced excitation level and frequency. Karagoz (1993) used a long exposure imaging method to investigate the unsteady flow near the point of bifurcation in a branching pipe. Ekmekci and Rockwell (2007) and Haigermoser (2009) have used particle image velocimetry (PIV) technique to visualize the oscillation of flow past a cavity, but their cavities were the

shallow free surface ($L < d$) systems. There was no acoustic field and the mechanism is totally different with the system which had long cavity ($L/d \gg 1$). Moreover, their experiments were performed in water channels. The velocities of the inflow velocity were much lower than that in this study.

In the present study, flow-induced acoustic resonance in a piping system containing closed side branches was investigated experimentally. The frequency of sound vibration was more than a few hundred Hz. The visualization method used in present experiment is the high time-resolved PIV technique. PIV is a non-intrusive measurement technique used to simultaneously determine the velocities at many points in a fluid flow. The instantaneous velocity fields were extracted using the recursive cross-correlation PIV technique. The dominant frequencies of the velocity fluctuation were analyzed by fast Fourier transform (FFT) analysis under conditions of different local mean velocities at the mouth of the cavity. The phase delay map in the visualization area was obtained from the analyzed velocity at the dominant frequency. This is the first two-dimensional experimental investigation to detect the time sequential instantaneous velocity field with long side branches ($L/D \gg 1$) and high inflow velocity at high resonant frequency.

2 Experimental setup

2.1 Experimental equipment

All the experiments were performed at the room temperature of 23°C in the laboratory. The experimental setup was designed to actualize direct observation of the flow in the cross-section of the side branch, and was shown schematically in Fig. 1. Ziada and Bühlmann (1992) have performed experiments of self-sustained pressure pulsations in pipes with closed side branches both for circular and square cross-sections. The experimental results showed that the pipes with square and circular section exhibited similar phenomena. Therefore, the present experiment setup was selected to be with rectangular section; the results can also be of benefit to systems involving pipes with other kinds of cross-sections.

The flow-generating unit consists of two pumps: The flow rate of each pump was controlled by a sonic nozzle. The mass flow meters were installed at the delivery end of each pump. The air coming from pump 1 flowed through an oil mist generator to form the working fluid. The air was seeded with oil mist particles (olive oil with a mean diameter of 3 μm) to visualize the fluid motion and the oil mist was generated by Laskin nozzle. Because the Stokes number was much smaller than 1, the particles could follow the fluid streamlines closely. Pump 2 was used to control the total mass flow rate and the number density of the particles in the working fluid. The total flow rate Q ranged from 25 to 54 l/min. In previous experiments, many researchers supplied a large mass flow in the main pipe to obtain a high mean velocity and a high shear flow velocity. Jungowski et al. (1989) have supplied mean velocity in the main pipe as $V = 51$ m/s and Reynolds number as $Re = (0.1–0.5) \times 10^6$ to excite the acoustic resonance. Ziada and Bühlmann (1992) have provided maximum flow rate of 2,000 m^3/h and maximum Reynolds number of 0.26×10^6 to

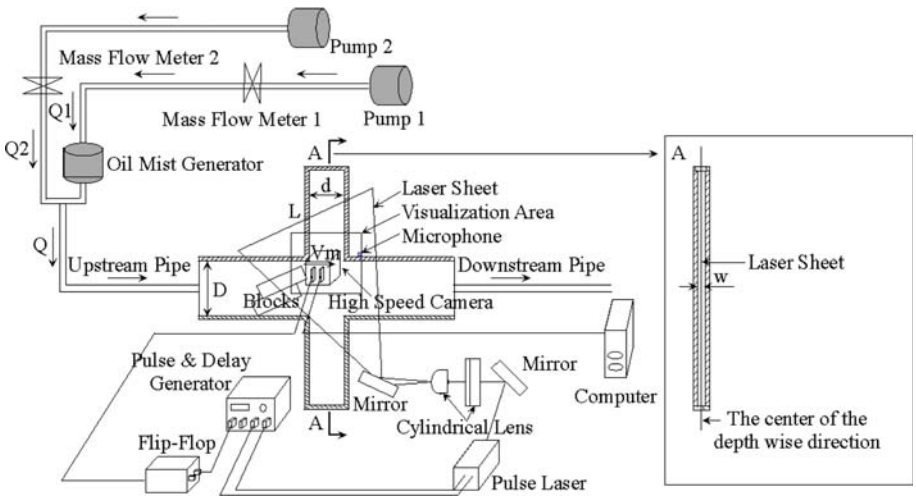

Fig. 1 Schematic representation of the experimental setup

the onset of resonance. In the present study, the experiments were done with high local mean velocity at the mouth of the cavity though the total mass flow rate was relatively smaller than those in other reports. The generation of the self-induced vibration with large amplitude needs high local mean velocity at the mouth of the cavity. To supply high-speed shear flow is more important than giving large mean velocity and large total mass flow in the main pipe. It is difficult to provide large mean velocity and large total mass flow due to the limitation of our pump system. Therefore, blocks were put at the upstream side of the cavity to form high local mean velocity at the mouth of the cavity in our system.

The coaxial side branches were made of rigid transparent acrylic resin in order to visualize the flow. All cross-sections of the main pipe were rectangular, with inner dimensions of 100×5 mm^2, namely, with $D = 100$ mm, $w = 5$ mm. The side branch pipes with inner dimensions of 25×5 mm^2 (i.e., $d = 25$ mm, $w = 5$ mm) and a length of 650 mm (i.e., $L = 650$ mm) were investigated. A SiSonic microphone (SP0103NC3-3 made by Dover Corporation) with integrated amplifier was put at 10 mm far from the downstream side of the upper closed side branch to detect the acoustical pressure. In addition, the two pipes forming the coaxial geometries were of equal length.

2.2 Optical arrangement

The two-dimensional velocity fields were measured using the PIV technique. A New Wave Research Pegasus-PIV laser ($\lambda = 527$ nm) was chosen to illuminate the test section. Two cylindrical lenses were used to produce a thin light sheet. One cylindrical lens with a focal length of 1,000 mm was used to make the laser sheet thin. In addition, the other cylindrical lens with focal length of 30 mm was used to expand the area of the laser sheet. The positions of the lenses were adjusted to produce a laser sheet about 1 mm in thickness and with a probing area of 35×17.5 mm^2. The laser sheet illuminated the visualization area at the incident angle of $-45°$ as shown in Fig. 1. The visualization plane was at the center of depth-wise direction.

A high-speed camera (FASTCAM-SA1.1, Photron Ltd.) captured the images of the particles at each pulse in the flow field. The light scattered by the oil mist particles inside the fluid in the direction perpendicular to the laser sheet was recorded on the high-speed camera to obtain particle images.

A pulse and delay generator was applied to synchronize the camera and the laser. A speed of 8,000 frames/s with a resolution of $1,024 \times 512$ pixels for the camera was selected. During each continuous run, a total of 21,837 PIV images were captured. From these 21,837 images, 10,918 velocity fields were processed and analyzed using the recursive cross-correlation PIV technique. For PIV cross-correlation, the initial interrogation size was 64×64 pixels and the last interrogation size was 32×32 pixels. The search window size was set equal to 26 and 20 pixels.

3 Results and discussion

The onset conditions of sound generation were investigated by the microphone by increasing the velocity little by little. Results are shown in Fig. 2. The frequencies of oscillation were calculated from the pressure fluctuation using FFT analysis. The black dots show the frequency in terms of the local mean velocity at the mouth of the cavity. The acoustical power of the frequency spectra was also dotted in gray in Fig. 2. The dashed line, which has a constant Strouhal number of 0.33, was obtained from connecting the black points that have the highest power spectrum of each mode except for the fourth mode. The two solid lines show a constant Strouhal number of 0.4 and 0.269, respectively, which are the highest and lowest Strouhal numbers at which resonance can occur in the present system.

The Strouhal number, St_{MIC}, is defined as

$$St_{\mathrm{MIC}} = \frac{f_{\mathrm{MIC}} d}{V_{\mathrm{m}}} \tag{1}$$

where f_{MIC} is the dominant frequency of the pressure fluctuation by FFT analysis, d is the width of the side branch, V_{m} is the local mean velocity at the mouth of the cavity. The Strouhal number became smaller as V_{m} increased for a certain acoustic mode. The Strouhal number is most important factor as describing the self-induced vibration. The present range of the Strouhal number agrees with typical St in cavity tones, edge tones (Arthurs and Ziada 2009; Dequand et al. 2003; Jungowski et al. 1989; Yang et al. 2009; Ziada and Bühlmann 1992).

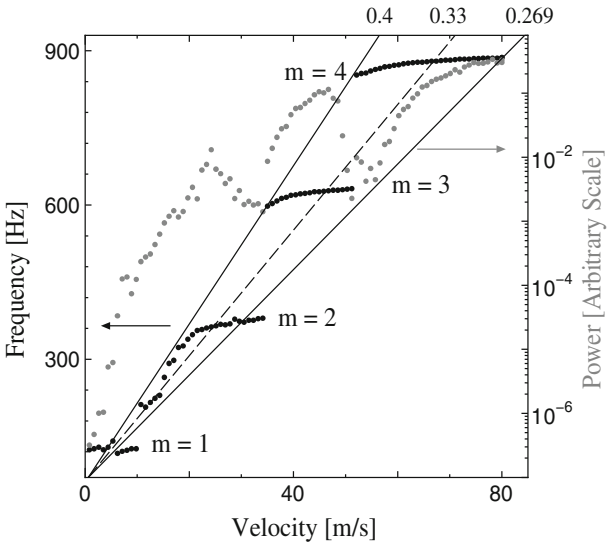

Fig. 2 Acoustical power (arbitrary scale) and frequency at the downstream side of the closed side branch in terms of the local mean velocity at the mouth of the cavity

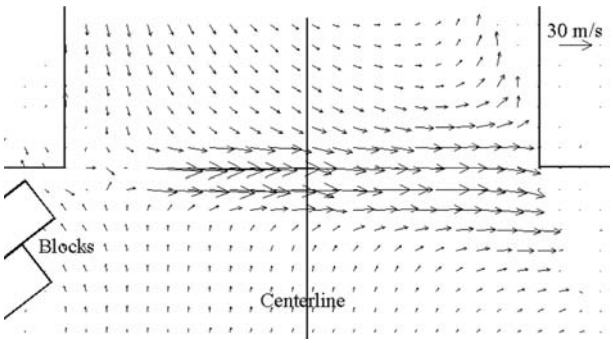

Fig. 3 Time-averaged velocity vector map for $Q = 30$ l/min. The vector on the *top right corner* indicates a magnitude of 30 m/s

It has been demonstrated in the literature, such as Ziada and Bühlmann (1992), that for piping systems with long side branches ($L/D \gg 1$) and large diameter ratios ($d/D \approx 1.0$), the resonance frequencies of the coaxial side branch modes at atmospheric pressure can be accurately predicted based on the length of the side branches, the speed of sound, and the diameter of the main pipe:

$$f_{\mathrm{CAL}} = \frac{C(2m-1)}{4(L+D/2)}, \quad m = 1, 2, 3, \ldots \tag{2}$$

where C is the speed of sound, the room temperature of the laboratory was always 23°C in this study, $C = 345.3$ m/s in this condition. L is the length of the branch, D is the height of the main pipe, m is the acoustic mode order. From this equation, when $m = 1$, 2, 3, 4, the frequencies of the acoustic modes are 123.32, 369.96, 616.61 and 863.25 Hz. These frequencies agree with the measured ones.

The PIV result of the time-averaged velocity vector map is presented in Fig. 3. The vector on the top right corner indicates a magnitude of 30 m/s. The local mean velocity at the mouth of the cavity obtained from this figure was 38.5 m/s. The black line displays the center of the branch. From this time-averaged velocity vector map, it may be seen that the vortex in the cavity is anticlockwise and the center of the vortex is on the right side of the centerline, i.e., near to the downstream side of the cavity. This result agrees with the numerical result obtained by Cheng and Hung (2006).

The instantaneous velocity vector fields during a period are presented in Fig. 4. The vector on the top right corner indicates a magnitude of 30 m/s. The time difference between the two successive velocity

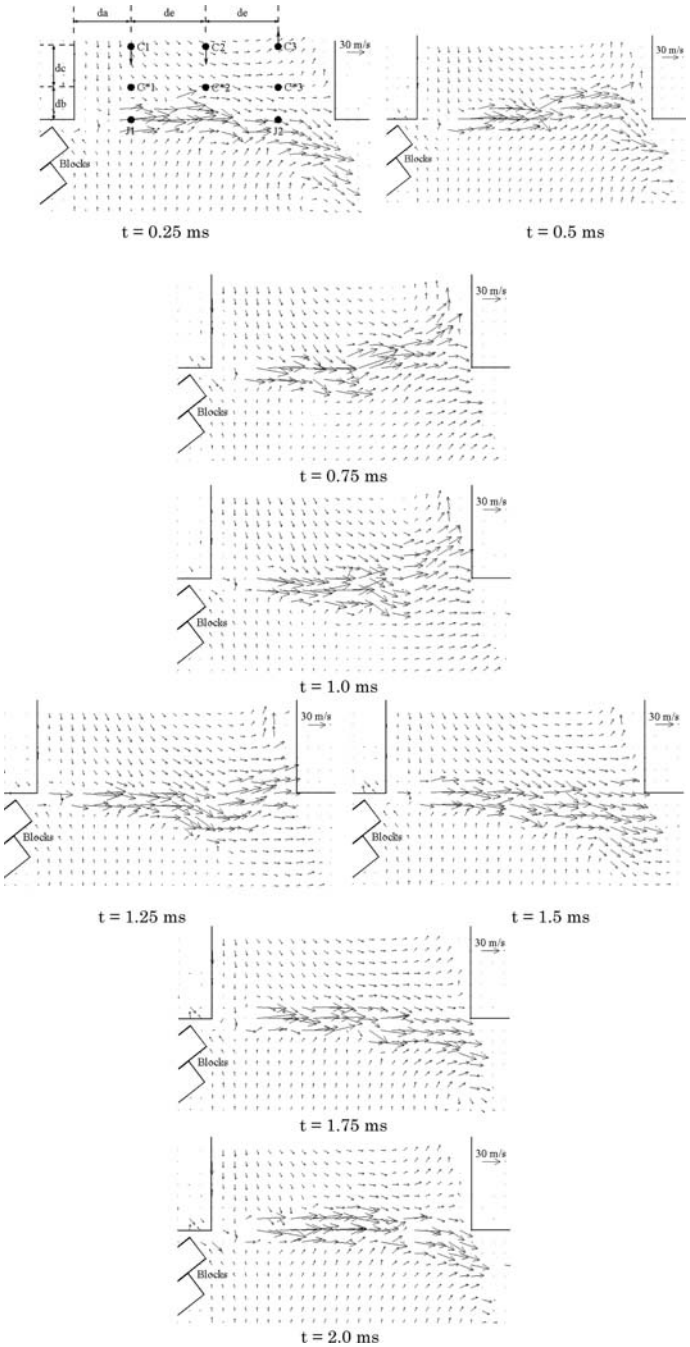

Fig. 4 Instantaneous velocity vector field for $Q = 30$ l/min at different times. The vector on the *top right corner* of each graph indicates a magnitude of 30 m/s

vector maps is 0.25 ms. The flow at the mouth of the cavity near the downstream side is downward at the first figure, then it moves upwards and downwards, with the period of cycling between 1.5 and 1.75 ms. That is to say, the rough estimate frequency is between 571 and 667 Hz.

Vertical component of the detected velocity vectors at different points in the cavity for $Q = 30$ l/min was shown in Fig. 5a. The parameters in Fig. 4 ($t = 0.25$ ms), da, db, dc and de, show the level of different points in the visualization area which have a range of da $= 0.217d$, db $= 0.131d$, dc $= 0.152d$ and de $= 0.283d$. The vertical velocity at point C3 (i.e., the point at the downstream side of the cavity) in the cavity always has a positive value. In other words, the vertical velocity at this point is always upwards,

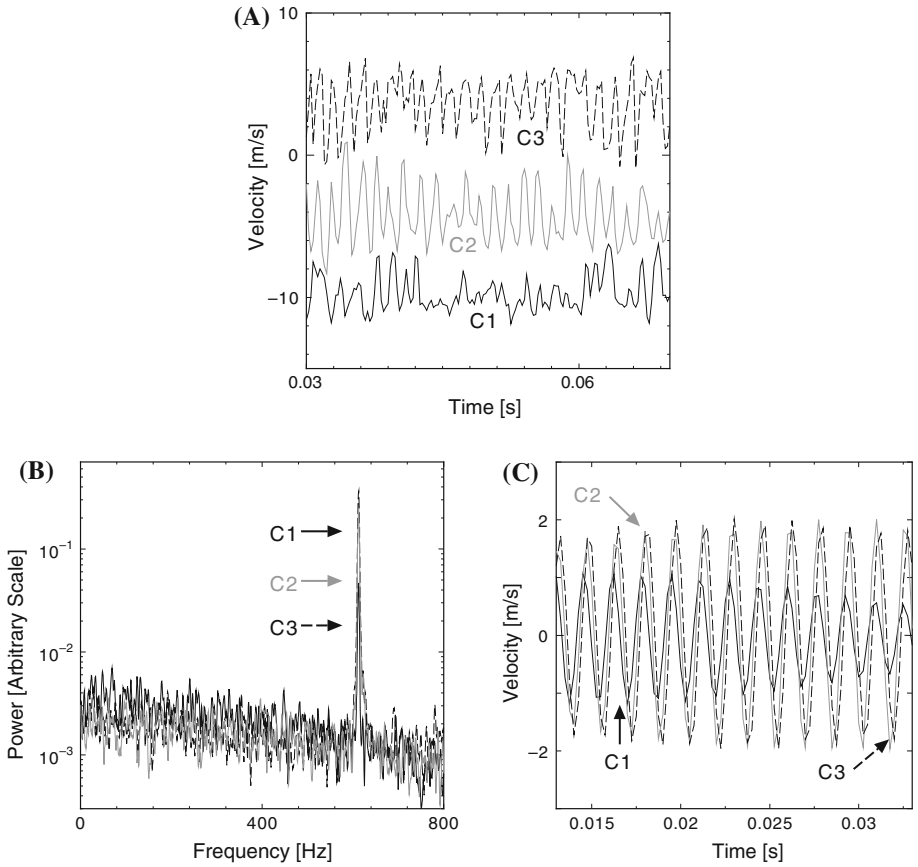

Fig. 5 Vertical velocity fluctuation and dominant frequencies of the velocity fluctuation by FFT analysis at different points in the cavity for $Q = 30$ l/min. The dominant frequencies of the velocity fluctuation by FFT analysis at different points in the cavity are about 613 Hz

expressed as upward arrows in Fig. 4 ($t = 0.25$ ms). On the other hand, the vertical velocities at points C1 and C2 (i.e., the points at the upstream side of the cavity) in the cavity always have negative values; i.e., the vertical velocities at these two points are always directed downwards, and are expressed as downward arrows in Fig. 4 ($t = 0.25$ ms). These results further prove that the vortex in the cavity near the cross-section is anticlockwise and the center of the vortex is on the right side of the centerline.

Figure 5b shows the dominant frequencies of the velocity fluctuation by FFT analysis (f_{PIV}) at different points in the cavity. From this figure, one can obtain the peak values, which are all about 613 Hz.

In this experimental condition, $m = 3$, the frequency estimated from Eq. 2 is 616.61 Hz, which is consistent with f_{PIV}. The difference between them is -0.585%.

From Fig. 2, when the local mean velocity was 38.5 m/s, f_{MIC} was equal to 614.26 Hz. The difference between f_{MIC} and f_{PIV} is -0.21%. The PIV experiment result is in good agreement with the result obtained from the microphone.

In this study, we have considered five different flow rates Q that correspond to five different local mean velocities at the mouth of the cavity V_{m} to excite the acoustic resonance in the cavity. The five different cases are summarized in Table 1. The Mach number, M, is defined as $M = V_{\mathrm{m}}/\mathrm{C}$; the dominant frequency of the velocity fluctuation by FFT analysis is expressed as f_{PIV}; the frequency estimated from Eq. 2 is expressed as f_{CAL}; the difference between the measured frequencies and that calculated from Eq. 2 is expressed as Ex; and the Strouhal number, St_{PIV}, is defined as $St_{\mathrm{PIV}} = f_{\mathrm{PIV}}d/V_{\mathrm{m}}$; the above all are listed in Table 1. From this table, it may be seen that the difference between f_{PIV} and f_{CAL} is below 3.145%.

Ziada and Bühlmann (1992) reported that there seems to be a minimum Reynolds number, or kinetic energy, which is required to excite the resonance, i.e., to achieve the lock-in phenomenon. In the present experiment, for $Q = 25$ l/min, there was only small peak at the cavity tone frequency in the power spectrum, shown in parentheses in Table 1.

Table 1 The cases considered for the acoustic experiments with the details of parameters for each case

Case	Q (l/min)	V_m (m/s)	M	f_{PIV} (Hz)	f_{CAL} (HZ)	Ex (%)	m	St_{PIV}
1	25	34.8	0.1008	(570)	616.61	(−7.559)	3	0.409
2	30	38.5	0.1115	613	616.61	−0.585	3	0.398
3	35	46.8	0.1355	627	616.61	1.685	3	0.335
4	41	51.5	0.1491	636	616.61	3.145	3	0.311
5	54	65.7	0.1903	878	863.25	1.709	4	0.334

Q flow rate, defined as Q1 + Q2; V_m the local mean velocity at the mouth of the cavity; M Mach number, defined as V_m/C; f_{PIV} dominant frequency of the velocity fluctuation by FFT analysis; f_{CAL} the frequency estimated from Eq. 2; Ex the difference between the measured frequencies and that calculated from Eq. 2; m the acoustic mode order; St_{PIV} Strouhal number, expressed in the form of $St_{PIV} = (f_{PIV})d/V_m$

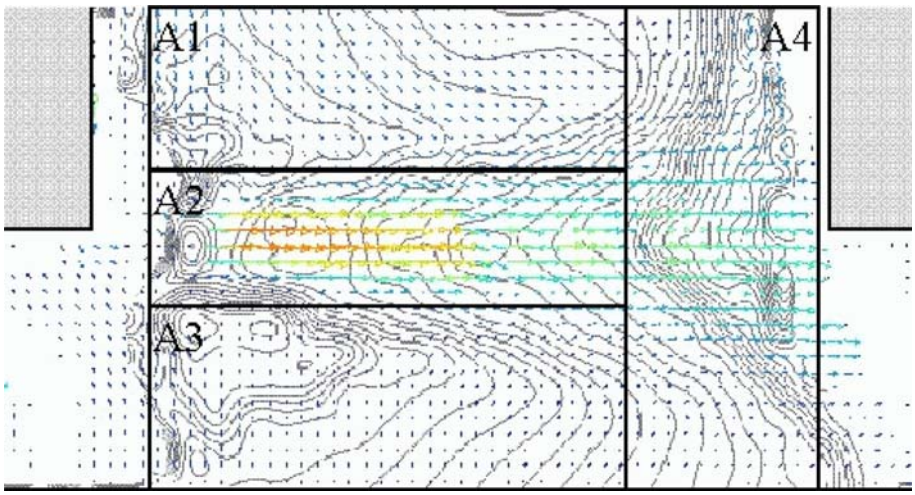

Fig. 6 Contour map of phase difference in the visualization area

The vertical component of the relative velocity fluctuations at different points in the cavity is shown in Fig. 5c. The vertical component of the relative velocity, V_r, is defined as

$$V_r = V_y - \bar{V}_y \tag{3}$$

where V_y is the vertical component of the detected velocity vector, $\bar{V}_y$ is the time-averaged value of the vertical component of the detected velocity vector at specific point. V_r was obtained by applying the band pass filter to V_y; hence, V_r reveals the velocity fluctuations at the frequency of cavity, and the amplitude of V_r was determined by that of the pressure fluctuation at that point. After using the band pass filter to cut off the high and low frequency (>630 Hz and <590 Hz), the phase difference between different points was shown clearly. According to this kind of figure, the phase difference between points C*2 and C*3 in Fig 4 ($t = 0.25$ ms) is 102.8°, between points C*2 and C*1 is 33.9°, between points C2 and C3 is 24.9°, and that between points C2 and C1 is 39.4°.

The phase difference at the mouth of the cavity between points J1 and J2 shown in Fig 4 ($t = 0.25$ ms) was 216.9°. The dominant frequency obtained from the PIV result was 613 Hz, so that the time delay between the two points was 0.98 ms. From the original image, the distance between the two points was 14.13 mm. Therefore, the propagation velocity of the fluctuation along the shear layer at the mouth of the cavity can be calculated to be $V_f = 14.42$ m/s. Meanwhile, the local mean velocity at the mouth of the cavity was $V_m = 38.5$ m/s, so that the fluctuation rate was $S = V_f/V_m = 0.375$. The Strouhal number in this condition was $St_{PIV} = 0.398$; the difference between S and St_{PIV} was 5.78%. This difference may be caused by the noise and error data within the original PIV results. At points J1 and J2 located at the mouth of cavity, the velocity was very high and its fluctuation was complicated.

The contour map of phase difference in the visualization area at the frequency of cavity is shown in Fig. 6. The contour interval is 10°. This figure was obtained from calculating the cross-correlation value for the vertical component of the relative velocity fluctuations at different points. This is the first research which

can obtain this kind contour map using the time sequential instantaneous velocity field. From this figure, one can obtain the phase difference between any two points. The phase delay between two points which keeps a certain distance in the upstream jet flow and in the cavity at A1, A2 and A3 is much smaller than that at A4. The phase delay at A4 becomes large dramatically. This indicated that the difference of vertical component of the relative velocity between two points which keeps a certain distance at the same time is larger in this area. Hence, the energy supply for oscillation in this area is larger than in other areas. The propagation of the velocity perturbation in the shear flow (i.e., in area A2) is slower than that in area A4. This suggests that the oscillating jet is affected by the structure of the downstream edge. Furthermore, this may imply that the shear flow near the trailing edge was deflected by the downstream edge and momentum was delivered into the branch. The phase difference contour line around the jet flow is nearly symmetry. However, the farther the points away from the shear flow, the more different the contour line becomes. The contour line in the cavity and in the main pipe is totally different, due to the existence of the side branch. This may imply that the impingement on the wall creates pressure perturbation supporting the acoustic field.

4 Summary and conclusions

In this report, an experimental investigation of flow-induced acoustic resonance in a piping system containing closed side branches was performed using the high time-resolved PIV technique. The present study of coaxial branches was the first rudimentary study to visualize the fluid flow in a cross-section and to measure the flow field two-dimensionally. A kind of self-induced vibration was observed in the cavity. Airflow containing oil mist as tracer particles was measured using a high-frequency pulse laser and a high-speed camera. The frequency of the sound vibration was generally a few hundred Hz, and the high time-resolved PIV makes it possible to measure the transient flow field at such a frequency and to clarify the flow interacting with the acoustic oscillation. In addition, the high time-resolved PIV clarified the relation between the flows at different points. Whenever comparison is possible, the present results are found to be in good agreement with the results reported by other researchers.

The results available from this initial investigation lead to the following conclusions:

The high time-resolved PIV technique can detect the time sequential instantaneous velocity field.
The results obtained from this experiment prove that the vortex in the cavity near the cross-section rotates in an anticlockwise direction and that the center of the vortex is at the downstream side of the cavity.
The dominant frequency and the phase difference were obtained from the PIV data. The measured frequency is in good agreement with the results obtained from the empirical equation and the microphone. The relation between sound propagation and flow field will be further estimated in a subsequent study.
The contour map of phase difference in the visualization area was obtained from calculating the cross-correlation value for the vertical component of the relative velocity fluctuations of different points. This is the first research which can obtain this kind contour map using the time sequential instantaneous velocity field. The results can illustrate the relation between the shear flow and the edge evidently.
The PIV technique can ascertain the fluctuation rate at the mouth of the cavity. The result is found to be in good agreement with the Strouhal number in this experimental condition.
Finally, we conclude that the high time-resolved PIV technique can be applied to high-speed gas flow in a cavity to measure the fluctuation transfer velocities.

Acknowledgments The authors would like to acknowledge the support of the Japan Ministry of Economy, Trade and Industry under the Innovative and Viable Nuclear Energy Technology (IVNET) Development Project.

References

Arthurs D, Ziada S (2009) Flow-excited acoustic resonances of coaxial side-branches in an annular duct. J Fluid Struct 25:42–59

Baldwin RM, Simmons HR (1986) Flow-induced vibration in safety valves. ASME J Press Vessel Technol 108:267–272

Bernstein M, Bloomfield W (1989) Malfunction of safety valves due to flow-induced vibrations. In: Au-Yang MK, Chen SS, Kaneko S, Chilukuri R (eds) Flow-induced Vibrations-1989, AMSE Publication No. 154. ASME, New York, pp 155–164

Bruggeman JC, Hirschberg A, Van Dongen MEH, Wijnans APJ, Gorter J (1989) Flow induced pulsations in gas transport systems: analysis of the influence of closed side branches. ASME J Fluid Eng 111:484–491

Cheng M, Hung KC (2006) Vortex structure of steady flow in a rectangular cavity. Comput Fluids 35:1046–1062

Coffman JT, Bernstein MD (1980) Failure of safety valves due to flow-induced vibration. ASME J Press Vessel Technol 102:112–118
Dequand S, Hulshoff SJ, Hirschberg A (2003) Self-sustained oscillations in a closed side branch system. J Sound Vib 265:359–386
East LF (1966) Aerodynamically induced resonance in rectangular cavities. J Sound Vib 3:277–287
Ekmekci A, Rockwell D (2007) Oscillation of shallow flow past a cavity: resonant coupling with a gravity wave. J Fluid Struct 23:809–838
Erickson DD, Durgin WW, Maquire CF, Moeller M (1986) Shear layer coupling with side-branch resonators. Forum on unsteady flow, ASME Publication No. FED 39, pp 43–45
Haigermoser C (2009) Application of an acoustic analogy to PIV data from rectangular cavity flows. Exp Fluid. doi: 10.1007/s00348-009-0642-5
Jungowski WM, Botros KK, Studzinski W (1989) Cylindrical side-branch as tone generator. J Sound Vib 131:265–285
Karagoz I (1993) Experimental investigation of periodic flow in branching pipes. Flow Meas Instrum 4(3):163–169
Kitajima Y, Watanabe M, Matsunaga K, Hagiwara T (2006) Acoustic analysis for a steam dome and pipings of a 1,100 MWe-class boiling water reactor. In: Proceedings of ICAPP'06, Paper 6358, Reno, NV, USA
Maguire CF III (1985) An experimental investigation of self-sustaining cavity oscillations in a pipe mounted side branch. Master thesis, Worcester Polytechnic Institute, Worcester, MA, USA
Rockwell D, Naudascher E (1978) Review-self sustaining oscillations of flow past cavities. ASME J Fluid Eng 100:152–165
Stoneman SAT, Hourgan K, Stokes AN, Weish MC (1988) Resonant sound caused by flow past two plates in tandem in a duct. J Fluid Mech 192:455–484
Yang Y, Rockwell D, Lai-Fook Cody K, Pollack M (2009) Generation of tones due to flow past a deep cavity: effect of streamwise length. J Fluid Struct 25:364–388
Ziada S (1994) A flow visualization study of flow-acoustic coupling at the mouth of a resonant side-branch. J Fluid Struct 8:391–394
Ziada S, Bühlmann ET (1992) Self-excited resonances of two side-branches in close proximity. J Fluid Struct 6:583–601
Ziada S, Shine S (1999) Strouhal numbers of flow-excited acoustic resonance of closed side branches. J Fluid Struct 13:127–142